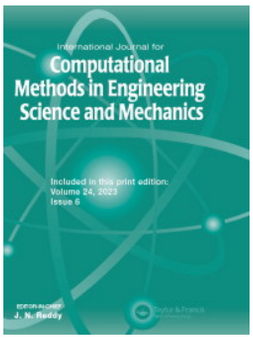

International Journal for Computational Methods in Engineering Science and Mechanics

ISSN: (Print) (Online) Journal homepage: www.tandfonline.com/journals/ucme20

Thermal tracking of a ladle during production cycles

Fredrik Berntsson & Patrik Wikström

To cite this article: Fredrik Berntsson & Patrik Wikström (2023) Thermal tracking of a ladle during production cycles, International Journal for Computational Methods in Engineering Science and Mechanics, 24:6, 406-416, DOI: 10.1080/15502287.2023.2253255

To link to this article: https://doi.org/10.1080/15502287.2023.2253255

INTERNATIONAL JOURNAL FOR COMPUTATIONAL METHODS IN ENGINEERING SCIENCE AND MECHANICS
2023, VOL. 24, NO. 6, 406–416
https://doi.org/10.1080/15502287.2023.2253255

Thermal tracking of a ladle during production cycles

Fredrik Berntsson[a] and Patrik Wikström[b]

[a]Linköping University, Linköping, Sweden; [b]Department of Metallurgical Development, SSAB Europe, Luleå, Sweden

ABSTRACT
Temperature control is important for the steel making process. Knowledge of the amount of thermal energy stored in the ladle allows for better predictions of the steel temperature during the process. This has a potential to improve the quality of the steel. In this work, we present a mathematical model of the heat transfer within a ladle during the production process. The model can be used to compute the current, and also the future, thermal status of the ladle. The model is simple and can be solved efficiently. We also present results from numerical simulations intended to illustrate the model.

KEYWORDS
Heat equation; steel making ladle; energy simulation; temperature control; industrial application

1. Introduction

Temperature control is an important factor during the steel production process in any steel plant. Knowledge of the correct actual steel temperature is important to give the correct treatment. The final steel temperature is dependent on many factors, such as tapping temperature, de-oxidation, and alloying. However, knowledge of the thermal condition of the ladle is also considered as an important factor throughout the steel making process.

Cold refractory lining will consume unnecessary energy from the steel and lower its temperature. Both too low and too high steel temperatures impose problems that could seriously jeopardize the final steel quality. Knowing which heats that need heating and which do not is thus very important. One solution is to monitor this through the use a tracking system that follows the history of the ladle [1,2]. Knowing the thermal status of the ladle makes it possible to adjust the tapping temperature to production needs.

The aim of this work is to present a mathematical model for the heat transfer that occurs in the ladle during the production. This includes the energy transfer from the molten steel into the ladle lining or to the lid, see [3], and also the preheater. The goal is to develop a numerical simulation code that allows us to calculate both the current and future thermal states of the ladle. Since the simulation software is intended to be used together with a real-time production planning system it is essential that the computation time is very short. The demand for computation speed means that a simple one-dimensional model is preferred.

The structure of our paper is as follows: In Section 2 we present our mathematical model of the ladle, including all the different ladle configurations that need to be considered. In Section 3 we show how to discretize the equations and organize the computations. Next, in Section 4 we perform numerical simulations intended to illustrate the properties of our model. In particular, we show the energy stored in the ladle during a realistic production cycle. Finally, in Section 5 we discuss our results and point out potential improvements.

2. The mathematical model of the ladle

In this section, we will describe our mathematical model of the ladle. The model covers all the different states of the ladle during a production cycle that starts with tapping, or possibly preheating, and ends with casting. We also discuss the initial drying of the ladle before its taken into production. In addition, we will discuss the assumptions, and simplifications, that we use to derive the model.

For the heat conduction in the wall and in the floor of the ladle, and also for the lid, we use the one-dimensional heat equation. Thus we introduce three different space variables $x^{(j)}$, $j = 1, 2, 3$, that describe the position in the wall, the floor, and the lid, respectively. In all cases $x^{(j)} = 0$ corresponds to the outside surface and $x^{(j)} = a_j$, see Figure 1, corresponds to the

CONTACT Fredrik Berntsson fredrik.berntsson@liu.se Linköping University, Linköping, SE-581 83, Sweden.

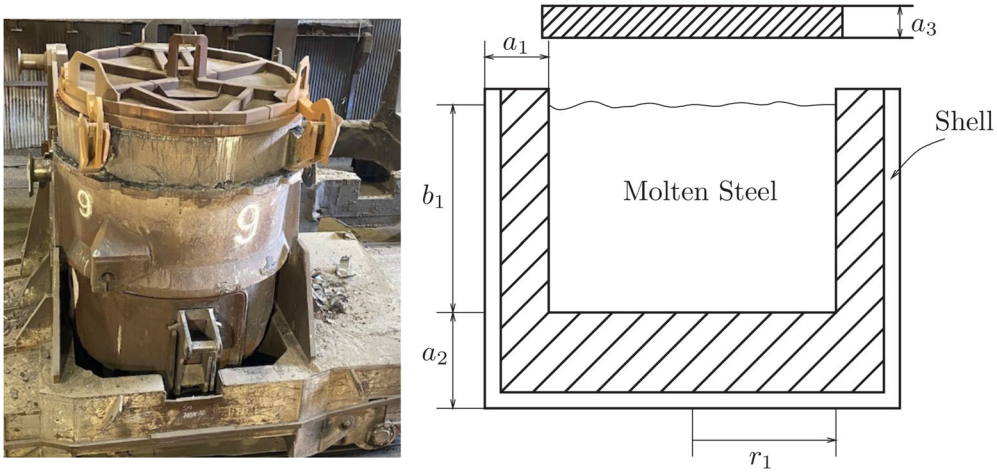

Figure 1. A full-sized ladle from SSAB (left). Also, a sketch showing the cross-section of the Ladle (right). The ladle is cylindrical and consists of an outer steel shell and various types of ceramic bricks. The interior is filled with molten steel. The important dimensions are the interior radius r_1, the thickness of the wall a_1, the thickness of the floor a_2, and the height b_1 which determines the volume of the molten steel in the interior. The lid has a thickness a_3.

interior where the interaction between the ladle and the molten steel occurs. The corresponding temperature profiles,

$$T^{(j)}(x^{(j)}, t), \quad 0 \le x^{(j)} \le a_j, \quad j = 1, 2, 3, \tag{1}$$

are assumed satisfy the one-dimensional heat equation, i.e.

$$\partial_x(k\partial_x T) = \rho c_p \partial_t T, \quad 0 < x < a, \ t > 0, \tag{2}$$

where k $[W/m\ K]$ is the thermal conductivity, c_p $[J/kg\ K]$ is the specific heat capacity, and ρ $[kg/m^3]$ is the density.

Note that for our application the ladle is built using several different materials and there is a large range of temperatures involved. Thus the material properties will depend on both position and temperature, e.g. $k := k(x, T)$. The material parameters for each of the materials are supplied from the manufacturer in the form of tables, e.g. $(T_i, c_p(T_i))$, and we use linear interpolation to find the appropriate parameter values to use when discretizing (2).

The molten steel is treated as a volume of constant temperature. This is justified by the much higher thermal conductivity of steel compared to the various ceramic materials that make up the ladle. Thus the model also includes the temperature $T^{(s)}(t)$.

The assumption that the one-dimensional heat equation accurately describes our situation can be justified as follows: The ladle wall consists of ceramic materials with a much lower thermal conductivity than the molten steel in the interior and the outer steel shell. Thus for the time scales involved it is reasonable to assume that both the shell and the molten steel have a constant temperature at a given instance of time. This means that the heat conduction in the wall and floor will only depend on the distance from the outer surface. This has also been verified, using both $2D$ calculations and measurements, in [1], for a similar case, see also [4].

We remark that by using the $1D$ assumption we effectively think of the Ladle as a disk of radius r_1 and thickness a_2, which represents the floor, that supports a cylinder with inner radius r_1, thickness a_1, and height b_1, see Figure 1. This is the material where the heat conduction takes place. In addition, we have the lid which consists of a circular disk with radius r_1 and thickness a_3. Thus the thermal energy content in the ladle is approximated by

$$E(t) \quad = 2\pi b_1 \int_0^{a_1} (r_1 + x^{(1)}) \left\{ \int_0^{T^{(1)}(x^{(1)}, t)} c_p(x^{(1)}, T)\rho(x^{(1)}, T) dT \right\} dx^{(1)} + \pi r_1^2 \int_0^{a_2} \left\{ \int_0^{T^{(2)}(x^{(2)}, t)} c_p(x^{(2)}, T)\rho(x^{(2)}, T) dT \right\} dx^{(2)}. \tag{3}$$

The energy can be computed rather efficiently by introducing an energy density function,

$$Q(T) = \int_0^T c_p(T)\rho(T) dT, \tag{4}$$

for each of the different material types used in the construction of the ladle. In our work, we construct a table $(T_i, Q(T_i))$, by numerical integration, and evaluate $Q(T)$ by linear interpolation. This means that the energy (3) can be computed efficiently. The choice of zero level for the thermal energy is of course rather arbitrary and in this work we define $E(t) = 0$ if the Ladle is at 0 °C.

2.1. Heat transfer coefficients

For each surface of the ladle, a boundary condition is needed. In our work, we model the net-energy flux across a surface and set a boundary condition of the type

$$q(t) = h(T_1, T_2)(T_1 - T_2), \tag{5}$$

where T_1 is the temperature at the surface, and T_2 either the ambient room temperature, typically denoted by T_∞, or the temperature of another surface. We consider both natural and forced convection, and also radiative heat transfer.

In the case of radiation heat transfer, we assign an emissivity γ to each surface and model the interaction with the background by [5]

$$\begin{aligned} q(t) &= h_r(T_1, T_\infty)(T_1 - T_\infty), \qquad h_r(T_1, T_\infty) \\ &= \sigma\gamma_1(T_1^2 + T_\infty^2)(T_1 + T_\infty), \end{aligned} \tag{6}$$

where σ is the Stefan-Boltzmann constant, and we have used the conjugate rule twice, i.e. $(a^4 - b^4) = (a^2 + b^2)(a + b)(a - b)$, to obtain the desired functional relationship (5). In the case of radiative heat transfer between two surfaces, with emissivity γ_1 and γ_2, respectively, we instead use

$$\begin{aligned} q(t) &= h_r(T_1, T_2)(T_1 - T_2), \qquad h_r(T_1, T_2) \\ &= \frac{\sigma(T_1^2 + T_2^2)(T_1 + T_2)}{\gamma_1^{-1} + \gamma_2^{-1} - 1}. \end{aligned} \tag{7}$$

The geometrical orientation, and areas, of the surfaces are taken into account by modifying the emissivity by suitable view factors [6].

In the case of natural convection across a surface, the situation is more complex. We compute both the Reynolds number and the Nusselt's number for the surface. Then we use the formulas in [6] to estimate the convection heat transfer coefficient $h_c(T_1, T_\infty)$. The combined heat transfer coefficient is then $h_1 = h_c + h_r$.

We illustrate the above by presenting the formulas for the convection heat transfer coefficient of the outer wall of the ladle. For the free convection, all temperature-dependent properties of air are evaluated at the temperature of the transition layer, i.e. $T_f = (T_1 + T_\infty)/2$. First, we compute the Reynolds number,

$$\mathrm{Re}_L = \frac{g\beta|T_1 - T_\infty|L^3}{\alpha\nu}, \tag{8}$$

where $L = b_1 + a_2$ is the characteristic length, $\beta = T_f^{-1}$ is the thermal expansion coefficient for the air, g is the gravitational constant, α is the thermal diffusivity, and ν is the kinematic viscosity, see [6, Eq. 9.25]. The Nusselt's number is then calculated by

$$\mathrm{Nu}_L = \left(\frac{0.825 + 0.387\mathrm{Re}_L^{1/6}}{(1 + (0.492/\mathrm{Pr})^{9/16})^{8/27}} \right)^2, \tag{9}$$

where Pr is the Prandtl number, and the expression is valid for a vertical surface [6, Eq. 9.26]. The free convection heat transfer coefficient is then calculated by

$$h_c(T_1, T_\infty) = \frac{\mathrm{Nu}_L k}{L}, \tag{10}$$

where k is the thermal conductivity of the air.

The same formulas are used for the inner-wall surface. A similar procedure, but using different formulas [6, Eq. 9.26], are used for the horizontally oriented surfaces, i.e. the lower and upper sides of the floor and the lid, and also for the surface of the molten steel contained in the ladle.

Example 2.1. To illustrate the above formulas we compute the combined heat transfer coefficient of the outer wall. During normal operation, the temperature of the outer steel shell of the ladle is at ~210 °C and the ambient room temperature is assumed to be 18 °C. This gives us a temperature $T_f = 114\ ^oC$. We recall that the above formulas are intended to be used with temperatures measured in K. The dimensions of the ladle we are modeling are such that the characteristic length is $L = 3.0\ m$. The properties of the air are taken from [6, Table A.4] and by inserting proper values in (8) we obtain the Reynolds number $\mathrm{Re}_L = 1.46 \cdot 10^{11}$. Inserting into (10) then gives the Nusselt's number $\mathrm{Nu}_L = 591.9$. Finally, the free convection heat transfer coefficient is $h_c = 6.46\ W/m^2\,^\circ C$.

For the radiation heat transfer coefficient, we assume that the outer steel shell has an emissivity of $\gamma = 0.95$. This gives the radiation heat transfer coefficient $h_r = 13.27\ W/m^2\,^\circ C$. The combined heat transfer coefficient for the outer wall is this $h = 19.37\ W/m^2\,^\circ C$. This means that at a temperature of 210 °C, the radiation heat transfer contributes the majority of the energy losses from the ladle. However, the free convection is not negligible and needs to be taken into account.

2.2. The slag model

The molten steel surface is not normally exposed to the air. Instead, there is a layer of slag material present [7,8]. The slag layer has thickness a_4, the material has a known thermal conductivity k_1, and the slag surface has a known emissivity γ_s. For our model, we do not solve the heat equation numerically inside the slag layer. Rather we use a simplified approach where

it is assumed that the slag layer is always at a steady state. This is justified by the fact that the slag layer is relatively thin.

Let $T^{(s)}$ be the temperature of the molten steel and let T_1 be the surface temperature of the slag layer. The steady state assumption means that the heat flux in the interior of the slag is a constant. The surface temperature of the slag can be computed by solving an equation that balances the thermal energy conducted through the slag against the energy flux from the surface of the slag. In the case when the lid is removed from the ladle we assume we have both radiation and free convection heat transfer and we solve the equation

$$g(T_1) = h_1(T_1, T_\infty)(T_1 - T_\infty) + k_1(T_1 - T^{(s)})/a_4, \tag{11}$$

where the combined heat transfer coefficient h_1, at the slag surface, is computed as described in Section 2.1 and T_∞ is the ambient room temperature.

If, instead the lid is attached to the ladle we assume that there is only radiation heat transfer between the lower surface of the lid and the slag. This means that the heat transfer coefficient is given by (7), where T_1 is the slag temperature and T_2 is the surface temperature for the lid. Thus we again obtain an equation similar to (11) to solve for the slag surface temperature.

Example 2.2. The effect of the slag can be illustrated by computing energy losses. First, for the case where the molten steel is directly exposed to the surroundings, we apply (6). With the assumption that the steel temperature is $T^{(s)} = 1650\ ^oC$, the ambient room temperature is 18 °C, and the emissivity is $\gamma = 0.5$, while recalling that the formulas are intended for temperatures in K, we obtain a radiation heat transfer coefficient $h_{r_1} = 237.49\ W/m^2\ K$. By using formulas from [6] for the case of a circular and horizontal surface we obtain a free convection heat transfer coefficient $h_c = 1.25\ W/m^2K$ for the same surface. Thus at these high temperatures, radiative heat transfer dominates.

For the case when a slag layer, of thickness $a_4 = 50\ mm$ and with a thermal conductivity $k = 3.0\ W/m\ K$, is present we first solve Eq. (11) to obtain the temperature $T_1 = 557.0\ ^oC$ on the surface of the slag layer. This much lower, temperature is then used to compute the radiative heat transfer coefficient for the surface $h_{r_2} = 40.5\ W/m^2\ K$.

The energy loss, for the molten steel, for the two cases can be computed as

$$Q_1 = A_s h_{r_1}(T^{(s)} - T_\infty) = 2.50\ MW \quad \text{and}$$
$$Q_2 = A_s h_{r_2}(T_1 - T_\infty) = 0.14\ MW,$$

where $A_s = 6.46\ m^2$ is the surface area of the slag layer. This is a substantial difference and demonstrates that including a model of the slag layer is important, see also [9] and [2, Section 4.2].

2.3. The molten steel model

The thermal conductivity of molten steel is relatively high compared to the materials that make up the rest of the ladle and the lid. Thus it is reasonable to treat the molten steel as a volume of constant temperature. For the interface between the molten steel and the wall and floor of the ladle we assume that the interior surface temperature of the ladle is the same as the temperature of the steel. This gives us boundary conditions,

$$T^{(j)}(a_j, t) = T^{(s)}(t), \quad j = 1, 2. \tag{12}$$

for the heat equation (2). The energy losses, by thermal conduction into the wall and floor, are computed by

$$q_j(t) = k_j A_j \partial_{x^{(j)}} T^{(j)}(a_j, t), \quad j = 1, 2, \tag{13}$$

where k_j, $j = 1, 2$, are the temperature-dependent thermal conductivities at the surface of the wall and floor, respectively, and A_j, $j = 1, 2$, are the area of the interior surfaces.

The energy loss through the upper surface of the steel depends on if the slag, see Section 2.2, is present or not. For the case when the slag is present we compute the surface temperature, T_1 of the slag, by formula (11), and can estimate the energy conducted through the slag layer by $q_3(t) = k_3 A_2(T_1 - T^{(s)})/a_4$. If there is no slag layer we instead compute a heat transfer coefficient, see Section 2.1, and estimate the energy loss to either the background or to the lid.

2.4. The different states

We recall that the purpose of the model is to track the thermal energy of the ladle during the production process. The ladle appears in different configurations that we need to model. We identify the following states:

1. Empty with no Lid.
2. Full with no Lid.
3. Empty with active burner.

4. Empty with Lid.
5. Full with Lid.
6. Tapping
7. Casting.

By making use of these states we can accurately describe the entire production cycle.

For all configurations described above the temperature profiles in the interior of the wall, floor, and lid, are assumed to satisfy the 1*D* heat equation. Also, the outside of the ladle and the upper side of the lid are always exposed to the surroundings. Recall that our coordinate systems are set up so that $x^{(j)} = 0,\ j = 1, 2, 3,$ correspond to the outside surface. Thus the energy transfer out from the Ladle, per unit area, can be written

$$q_j(t) = h_j(T^{(j)}(0, t) - T_\infty), \quad j = 1, 2, 3, \tag{14}$$

where the heat transfer coefficients h_j, are temperature dependent and are computed as discussed in Section 2.1.

The *Empty/No Lid* state is the simplest one. Here we compute three heat transfer coefficients: for the inner wall, the upper floor, and the lower lid. We also compute suitable view factors that allow us to accurately compute the net energy loss from these surfaces to the surroundings. We remark that while the lid is not attached to the ladle it is still part of the model. Similarly, the temperature of the molten steel $T^{(s)}(t)$ is included in the model, and for the case of an empty ladle we keep $T^{(s)}(t) = 0$.

For the *Full/No Lid* state we have the energy loss through thermal conduction from the steel into the wall and floor of the ladle. We also assume that the slag layer is present. By computing the slag temperature, as described in Section 2.2, we can compute the total energy loss for the molten steel. Again the Lid is included in the model and we compute an appropriate heat transfer coefficient for the lower side of the lid.

The two states *Empty/With Lid* and *Empty/With Burner* are very similar in the sense that for both states the steel temperature is kept at $T^{(s)}(t) = 0$ and the steel does not interact with the rest of the ladle. Also, we assume that the heat transfer between the three surfaces (inner wall, upper floor, and lower lid) is dominated by the radiation. We compute temperature-dependent, heat transfer coefficients $h_j,\ j = 1, 2, 3,$ and the necessary view factors, accordingly. For our case, the view factors are taken from [6, Problem 13.7]. In the case of an active burner, we add an extra energy influx of the type $q_j = h_g(T^{(j)} - T_g)$, where T_g is the gas temperature and h_g is a forced convection heat transfer coefficient. The heat transfer coefficient h_g is not calculated using theoretical results but rather selected experimentally so that the model agrees with measured temperature curves. For a more detailed study of the preheater see [10].

The *Full/With Lid* state consists of thermal conduction from the molten steel into the wall and floor of the ladle. Again we compute the slag temperature T_s by solving (11). This allows us to compute the energy loss for the molten steel, and also the net influx into the lid. The interaction between the slag layer and the lower lid surface is assumed to be entirely due to radiation heat transfer. There is no view factor used for this state since the areas are identical and the lid is positioned reasonably close to the molten steel.

The *Tapping* state is difficult to model accurately using 1*D* heat conduction. In our work, the ladle is filled instantly. The lid is not attached to the ladle during the process. The difference compared to the *Full/No Lid* state is that the slag layer is not yet present. Instead, a radiation heat transfer coefficient is computed for the upper surface of the molten steel. This leads to much larger energy loss for the duration of the tapping stage. Since the tapping stage is relatively short in time we do not expect the errors introduced here to influence the overall results.

Finally, the *Casting* stage is also difficult to model accurately using a 1*D* model. In our model, this stage is considered identical to the *Full/With Lid* state. The slag is present, which limits the loss of thermal energy. We do not know exactly at which rate the ladle is emptied of liquid steel. Thus we cannot accurately compute the temperature of the steel during this stage. This will of course also introduce errors in the temperature profiles of the ladle walls and floor. Since the casting stage takes more time, compared to the Tapping, there is a larger potential to introduce errors here. This will be further discussed in Section 4, where we present our numerical results.

3. The numerical model

The numerical method is based on the idea of treating space and time discretization separately. First, we deal with the space discretization. Introduce a step size Δx and also three different uniform grids $\{x_i^{(j)}\}$, $0 = x_1^{(j)} < x_2^{(j)} < \ldots < x_{n_j}^{(j)} = a_j, \quad j = 1, 2, 3,$ for the wall, floor, and the lid. We also introduce the unknown temperatures in the form of vectors,

$$T^{(j)}(t) = (T^{(j)}(x_1^{(j)}, t),\ \ldots, T^{(j)}(x_{n_j}^{(j)}, t))^T, \quad j = 1, 2, 3. \tag{15}$$

In addition, we have the temperature of the molten steel, i.e. $T^{(s)}(t)$. The unknowns are collected in a vector $V(t)$, i.e.

$$V(t) = (T^{(1)}(t),\ T^{(2)}(t),\ T^{(3)}(t),\ T^{(s)}(t))^T, \tag{16}$$

of length $n = n_1 + n_2 + n_3 + 1$. The goal of the space discretization step is to write the time derivative of $V(t)$ in the form,

$$\partial_t V(t) = AV(t) + b, \tag{17}$$

where $A := A(V(t))$ is an $n \times n$ matrix that depends on the current temperature distribution inside the ladle, and $b := b(V(t))$. In the next few subsections, we describe in detail how the matrix A and the vector b is to be computed.

The purpose of formulating the space discretization in the form (17) is that we can use any standard time stepping technique. In our work, we prioritize simplicity, and computational speed, and use the backwards-Euler scheme. Thus, we discretize the time derivative as

$$\frac{1}{\Delta t}\big(V(t_j) - V(t_{j-1})\big) = AV(t_j) + b, \tag{18}$$

where the non-linearity is dealt with by computing the matrix A, and the vector b, using the previous thermal distribution $V(t_{j-1})$ of the ladle. Thus, we need to solve a linear system of equations,

$$V(t_j) = (I - \Delta t A)^{-1}(V(t_{j-1}) + \Delta t b), \tag{19}$$

for each time step t_j. The time step Δt is selected so the errors introduced by this approximation are negligible compared to other modeling errors.

3.1. Interior points and the molten steel

The interior points inside the wall, floor, or lid, do not depend on the state of the ladle. Thus all three sets of variables, $T^{(j)}(t)$, $j = 1, 2, 3$, are treated in the same way. For simplicity, we drop the superscript (j) in the rest of this section.

Note that the variables $T(x_{n_j}, t)$ and $T(x_1, t)$, located on the surfaces, do indeed depend on the current state of the ladle and have to be left out for now.

Firstly, we evaluate the material properties for the current temperature distribution $T(x_i, t)$, and obtain the thermal conductivity, density, and specific heat capacity at each grid point, e.g. $k_i := k(x_i, T(x_i, t))$. At interior points the heat equation (2) holds, and the standard symmetric finite difference approximation is,

$$(\rho c_p)_i \partial_t T_i(t) = \frac{k_{i-1/2}T_{i-1}(t) - (k_{i-1/2} + k_{i+1/2})T_i(t) + k_{i+1/2}T_{i+1}(t)}{\Delta x^2}, \tag{20}$$

for $i = 2, 3, \ldots, n_j - 1$, and where half-index points are calculated using linear interpolation.

The molten steel is treated as a uniform volume with a constant temperature $T^{(s)}(t)$. The interaction between the steel and the ladle happens at the boundaries, i.e. the inner wall and the upper floor. Here we assume that the respective surfaces have the same temperature as that of the molten steel, i.e. $T^{(j)}_{n_j}(t) = T^{(s)}(t)$, $j = 1, 2$. The corresponding energy loss is computed by,

$$\begin{aligned} Q_j(t) &= A_j k_{n_j} \partial_x T(x_{n_j}, t) \\ &\approx A_j k_{n_j} \frac{3T_{n_j}(t) - 4T_{n_j-1}(t) + T_{n_j-2}(t)}{2\Delta x}, \end{aligned} \tag{21}$$

for $j = 1, 2$, where A_j are the area of the inner wall and the upper floor, respectively, and the k_{n_j} are the thermal conductivity at the surface grid point.

The energy loss at the upper surface of the steel depends on if the slag layer is present or not. The details are explained in Section 2.3. There are no further numerical approximations for this surface and we can compute the energy loss $Q_3(t)$ across the upper surface of the molten steel.

The combined energy loss is then used to the time derivative of the steel temperature by

$$V_s \rho c_p \partial_t T^{(s)}(t) = -Q_1(t) - Q_2(t) - Q_3(t), \tag{22}$$

where the density ρ and specific heat c_p of the steel are temperature-dependent and V_s is the volume of the molten steel.

For the case when the ladle is empty we simply use $\partial_t T^{(s)}(t) = 0$. The temperature of the steel is also set at the beginning of the tapping phase and at the end of the casting phase.

3.2. Implementation of boundary conditions

In the previous section, we discussed the interior points in the wall, floor, and lid, and also the interface between the ladle and the molten steel, for the case when the ladle is full. We have also explained how to deal with the upper surface of the molten steel. This leaves the surfaces of the lid, the outer wall, lower floor, and, for the case of an empty ladle, also the inner wall and upper floor. For all these surfaces we have convection heat transfer.

We illustrate the implementation of a convection boundary condition by considering the outer wall

surface. The aim is to compute the time derivative of the temperature at the surface grid point x_1, i.e. $\partial_t T_1(t) := \partial_t T(x_1, t)$. We consider the net energy influx, per unit area and unit time, to a finite volume of width Δx, located at the outer surface, and obtain

$$Q(t) = k_1 \partial_x T(x_1, t) - h_1(T(x_1, t) - T_\infty), \tag{23}$$

By discretizing the derivative using a one-sided difference quotient, we find that the change of temperature, per unit area, in the finite volume is

$$(\rho c_p)_1 \partial_t T_1(t) \approx$$

$$\frac{1}{\Delta x}\left(k_1 \frac{-3T_1(t) + 4T_2(t) - T_3(t)}{2\Delta x} - h_1(T_1(t) - T_\infty)\right), \tag{24}$$

where, as previously, the material properties ρ, c_p, and k, at the grid point x_1, are temperature dependent. The remaining surfaces are treated in a similar way.

4. Simulated numerical examples

In this section, we present numerical results obtained by using our code. The ladle model contains too many physical parameters to present in detail. The most important ones are the inner radius $r_1 = 1.43\ m$, the wall thickness $a_1 = 0.266\ m$, the wall height, $b_1 = 2.50\ m$, the floor thickness $a_2 = 0.506\ m$, the thickness of the lid $a_3 = 0.150\ m$, and the thickness of the slag layer $a_4 = 5\ cm$. Also, for the preheater, e.g. the *Empty/With burner* state, we assume a gas temperature of $1250\ ^\circ C$ and a forced convection heat transfer coefficient $h_g = 183\ W/m^2\ ^\circ C$.

For all tests, we used the step size $\Delta x = 0.2\ mm$ in space and $\Delta t = 10\ s$ in time. The computations were carried out using Matlab.

Test 4.1

In our first test, we compute a steady state temperature distribution in the wall and the floor of the ladle. This is done under the assumption that the ladle is filled with steel, which is kept at a constant temperature $T^{(s)} = 1650\ ^oC$. We display the results in Figure 2. In both cases, the temperature on the outside surface is ~200 °C. The larger thickness of the floor, which should result in a lower surface temperature, is counteracted by the smaller free convection heat transfer coefficient due to the surface being horizontal. We also compute the thermal energy contained in the ladle by evaluating the formula (3) and obtain $E_s = 36.86\ GJ$. It is interesting to note that the temperature is close to constant in the outer steel shell.

Test 4.2

In the second test, we illustrate the effect of the slag layer. Starting from a situation where the ladle is at a steady state, i.e. the temperature distribution seen in Figure 2 we run a simulation with *Tapping*, for 5 min, followed by the *Full/No Lid* state for 45 min. The results are shown in Figure 3. Here we have implemented two versions of the *Full/No Lid* state: with or without the slag layer. In both cases, we display the steel temperature $T^{(s)}(t)$. Note that for the tapping state, there is no slag. The difference in the final steel temperature between the two simulations is about 72 °C. This clearly illustrates the insulating properties of the slag.

Similar simulations using the *Full/With Lid* state are also presented. For this case, the difference in the steel temperature, at the end of the casting, is about 6 °C. We also display the corresponding temperatures $T^{(3)}(x_{n_3}, t)$ on the lower surface of the lid. For this simulation, the initial temperature of the lid was constant 18 °C. We see that including the slag layer in the model has a significant impact on the temperature in the lid.

For the next few tests, we introduce a realistic cycle for the ladle during the production process. The cycle is as follows: Initially, the ladle is in a waiting state before its used in production. Here we assume that the initial waiting period lasts for 70 min. The lid is not necessarily attached during this period. Next, the ladle is moved to a preheater for 15 min in preparation for the tapping, which lasts for 6 min. The lid is attached directly after tapping and the ladle is transported to a treatment station, and on to casting. The entire process, including waiting time, is about 90 min and the actual casting lasts for about 45 min. After the casting the ladle returns to the initial waiting stage. Here there is transport, waiting time, and possibly maintenance done on the ladle. The production cycle is displayed in Table 1. The entire cycle lasts for 246 min.

Test 4.3

For the third test, we started by running the preheater for 8 *h*, starting from the ladle was at a constant 18 °C. After the initial preheater step the ladle has 18.1 *GJ* of thermal energy stored. Then we repeat *Cycle 1*, see Table 1, until we reach a steady-state. For

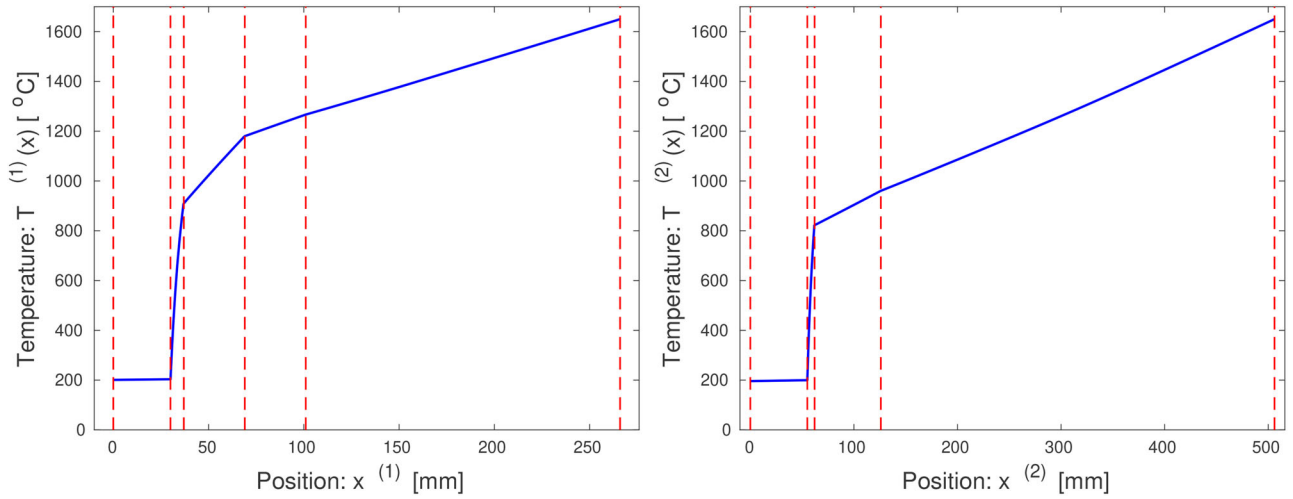

Figure 2. The steady-state temperature distribution in the wall (left graph) and the floor (right graph). In both cases, the steel is kept at a constant 1650 °C. The different materials are illustrated by vertical lines (red dashed) that show where the material changes. The material types in the wall are in order (left to right in the graph): outer steel shell, insulation cloth, insulation lining, safety lining, and working lining. For the floor, it is an outer steel shell, insulation cloth, safety lining, and working lining.

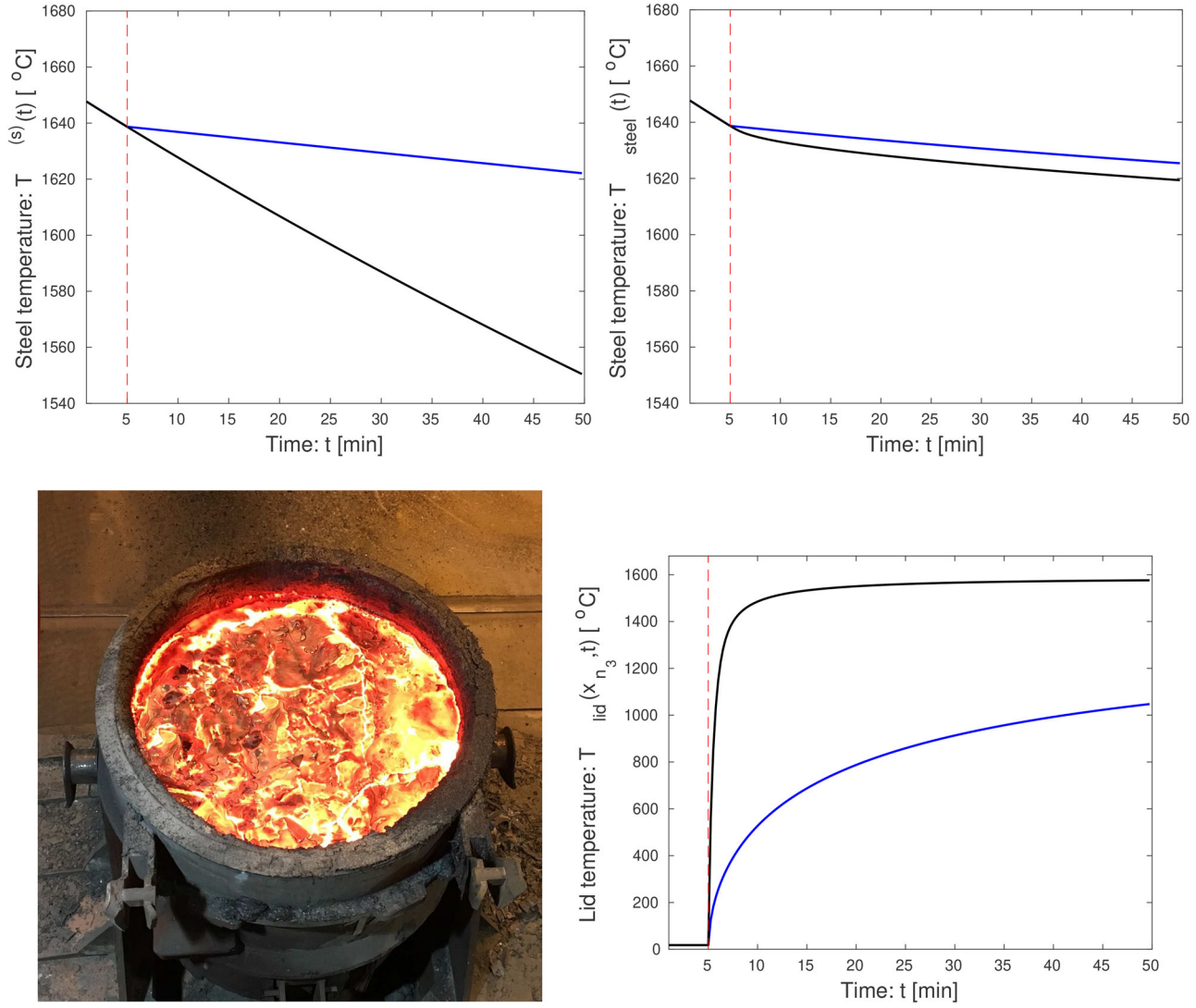

Figure 3. The cooling of the steel $T^{(s)}(t)$ for the case without the lid (top-left). We also show the steel temperature $T^{(s)}(t)$ for the case when the Lid is present (top-right) in the simulation. In both cases, we show the results with the slag layer (blue curves) and without the slag (black curves). For the latter case, we also show the temperature $T^{(3)}(x_{n_3}, t)$, on the lower surface of the lid (lower-right). We also show a photo of the ladle, without the lid, so that the hot slag layer is visible (lower-left).

this experiment repeating the cycle 15 times is sufficient. After having reached steady-state we run both production cycles once each and display the results in Figure 4. Note that the difference between the two cycles is in the initial waiting, period before the tapping, where the lid does reduce the thermal losses.

It is interesting to note that for the case when the lid is attached, during the initial 70 min of waiting time, the interior surfaces of the ladle are warmer than the hot gas used by the preheater. Thus the ladle is actually losing energy. The difference in stored thermal energy between the two cases, at the start of tapping is 2.2 *GJ* and the resulting difference in steel temperature at the end of casting is 18 °C. This is a significant difference.

Test 4.4

For the final test, we investigate how the final temperature of the steel, at the end of the casting phase, depends on the thermal energy stored in the ladle at the start of the tapping phase. The simulation is carried out as follows: A steady state temperature distribution, for the ladle, is created by running the preheater for 8 *h*, followed by *Cycle 1*, see Table 1, 15 times. Finally, we run both production cycles one more time, but with the initial waiting time changed, from 70 min, to between 0 and 540 min. The initial waiting time determines the thermal energy stored in the ladle at the start of tapping. This in turn influences the cooling rate for the molten steel. We recall that the steel is always at 1650 °C at the beginning of the tapping phase. The results are shown in Figure 5.

We remark that thermal energy is stored in the lid, but this is not included in the energy calculation, see (3), for the ladle. In our simulation model, the lid is cooled by convection if it is not attached to the ladle. This means that if the initial waiting period is without the lid present, then it will have a lower temperature when it is reattached after tapping. This means that the lid will absorb more thermal energy from the molten steel by radiation heat transfer. This is seen in Figure 5. The energy content in the lid is not insignificant and influences the results.

Table 1. The assumed production cycles for our numerical simulation.

State/Cycle 1	E/NL	E/B	TAPP	F/WL	CAST	E/WL
State/Cycle 2	E/WL	E/B	TAPP	F/WL	CAST	E/WL
Time (min)	70	15	6	90	45	20

5. Concluding remarks

In this paper, we have presented a mathematical model of the energy transfer in a ladle, used for steel production. The model is one-dimensional and calculates the time-dependent temperature distribution inside the ladle wall and floor, and also inside the lid.

The purpose of our simulation model is to track the thermal energy in the ladle. This is important since the temperature distribution of the ladle influences the energy losses for the steel between the tapping and casting steps. If the temperature of the ladle drops below a certain threshold we can use the preheater, to add thermal energy to the ladle, before tapping. Thus we use our mathematical model in two ways: First to compute the current temperature distribution of the ladle, by taking into account its unique history, and

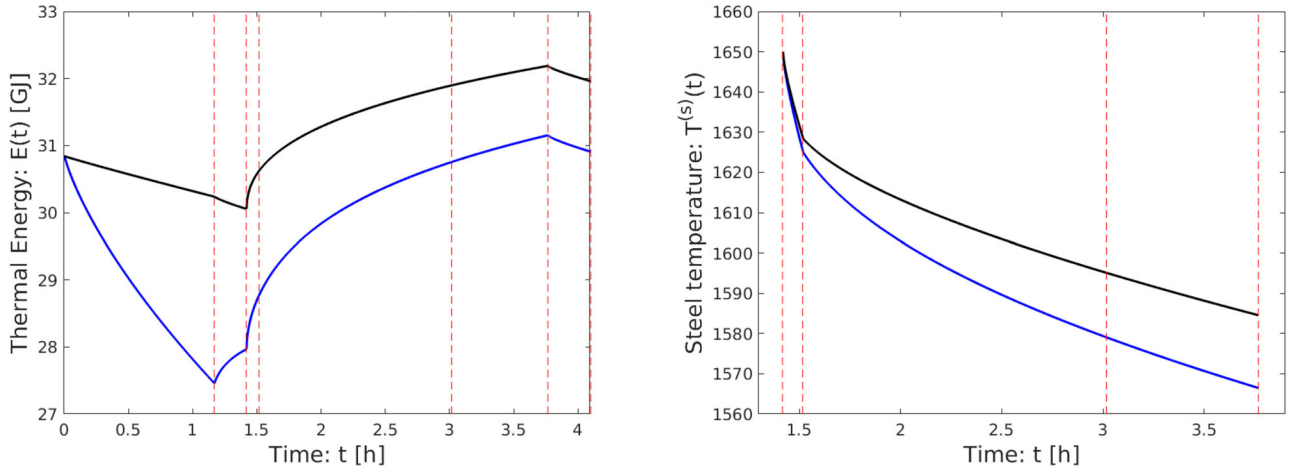

Figure 4. The simulation results for the simple production cycle. We display the thermal energy stored in the ladle in the two production cycles (left). Also, we show the steel temperature $T^{(s)}(t)$, from the start of tapping to the end of casting (right). In both cases we show the results for *Cycle 1* (blue curves) and for *Cycle 2* (black curves). The vertical lines (red-dashed) indicate the times when the ladle configuration changes.

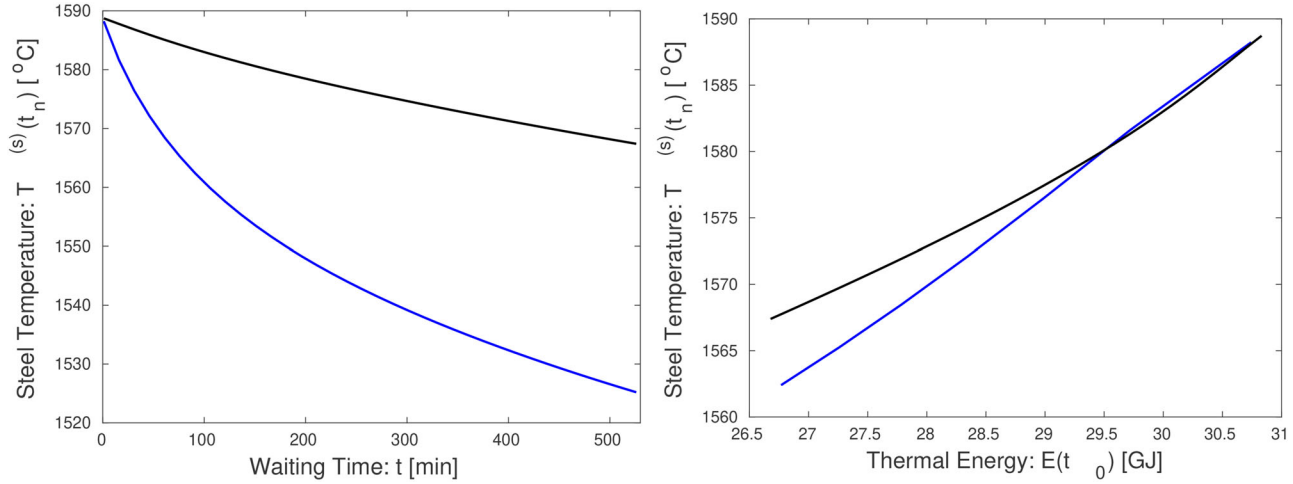

Figure 5. We display the final temperature of the molten steel at the end of the casting step, as a function of the time spent, in the *Empty/With Lid* state, waiting for tapping to begin (left graph). We also show the final steel temperature as a function of the thermal energy, stored in the ladle, when the tapping begins (right graph). As previously, the results for *Cycle 1* (blue curves) and for *Cycle 2* (black curves) are shown.

also to predict a future thermal state for the ladle by making assumptions about the ladles scheduled path from tapping to casting. This way we can ensure a desired temperature for the molten steel during the casting. Also, the lid has an interior temperature distribution and thus stores thermal energy. In our model, the lid is tracked together with the ladle. However, in practice, it would make more sense to track the ladles and the lids separately. This is also something we will consider in the future.

The advantage of using a one-dimensional model is computation speed. With grid parameters $\Delta x = 0.2\ mm$ and $\Delta t = 15\ s$ our code requires $\sim$23.8 s of runtime, per hour of simulation time, when using Matlab on an HP Desktop, with an Intel Xeon 3.7 GHz processor. Increasing the step size to $\Delta x = 1\ mm$, which still gives very good accuracy, we instead need 4.9 s for each hour of simulation time. The computational efficiency is important since we intend to use our model together with the production control system at SSAB for real-time monitoring of the different ladles that are in use.

The downside of using the one-dimensional heat equation is that we cannot accurately model the tapping or casting steps. The tapping state is relatively short and isn't likely to introduce any large errors, but the casting lasts for a longer period of time and needs further investigation. However, it is important to realize that errors in our numerical model cannot accumulate over time. This is because thermal energy is only added to the system by the preheater, or with the molten steel during the tapping. The temperatures inside the ladle cannot exceed that of the molten steel. Also, a too high, or too low, temperature in the ladle will lead to larger, or smaller, thermal losses by convection at the outer surfaces. This will automatically compensate for errors in other parts of the simulation.

In addition to the states identified, and described, in Section 2.4 we have the Treatment of the steel. This is similar to *Full/With Lid* but the treatment process can add, or remove, thermal energy. A *Treatment* state could be implemented in our model by adding a term $Q_4(t)$ to the energy balance equation (22) for the molten steel. This is something we have not yet done.

The numerical simulations presented in this paper show that the model works as expected, and the results are realistic. We have also verified the results by comparing them with finite element calculations. It has proven difficult to make more detailed comparisons with other published work, e.g. [2,4]. This is because our focus has been on implementing a model of the specific ladle used by SSAB. Thus, results from the literature are for different ladles. It has also proved challenging to find realistic parameters for a few of the materials in the model. In particular for the insulation cloth used in the walls and the floor. The data supplied by the manufacturer is likely not correct. In the future, we plan to make an experimental study of the temperatures in a ladle during the production process, in an actual steel mill, and use the results to adjust the parameters of our model.

Disclosure statement

No potential conflict of interest was reported by the author(s).

ORCID

Fredrik Berntsson http://orcid.org/0000-0002-2681-8965

References

[1] S. Ferro, C. Cicutti, and P. Galliano, "Thermal Tracking of Ladles," Proceedings of the 8th International Conference on Modeling and Simulation of Metallurgical Processes in Steelmaking. Association for Iron & Steel Technology, 2019, pp. 241–247.

[2] A. Tripathi, J. K. Saha, J. B. Singh, and S. Kumar Ajmani, "Numerical simulation of heat transfer phenomenon in steel making ladle," *ISIJ Int.*, vol. 52, no. 9, pp. 1591–1600, 2012. DOI: 10.2355/isijinternational.52.1591.

[3] O. Volkova and D. Janke, "Modelling of temperature distribution in refractory ladle lining for steelmaking," *ISIJ Int.*, vol. 43, no. 8, pp. 1185–1190, 2003. DOI: 10.2355/isijinternational.43.1185.

[4] C. E. Grip, L. Jonsson, P. Jönsson, and K. O. Jonsson, "Numerical prediction and experimental verification of thermal stratification during holding in pilot plant and production ladles," *ISIJ Int.*, vol. 39, no. 7, pp. 715–721, 1999. DOI: 10.2355/isijinternational.39.715.

[5] J. P. Holman. *Heat Transfer*, 10th ed. New York, NY: McGraw Hill, 2010.

[6] T. L. Bergman, A. S. Lavine, F. P. Incropera, and D. P. DeWitt. *Fundamentals of Heat and Mass Transfer*. Hoboken, NJ: Wiley, 2011.

[7] B. Glaser and D. Sichen, "Thermal conductivity measurements of ladle slag using transient hot wire method," *Metall. Mater. Trans. B*, vol. 44, no. 1, pp. 1–4, 2013. DOI: 10.1007/s11663-012-9773-9.

[8] K. Youngjo, L. Joonho, and M. Kazuki, "Thermal conductivity of molten slags: a review of measurement techniques and discussion based on microstructural analysis," *ISIJ Int.*, vol. 54, no. 9, pp. 2008–2016, 2014.

[9] Y. Dong, Z. Jiang, Y. Cao, D. Hou, L. Liang, and J. Duan, "Effective thermal conductivity of slag crust for ESR slag," *ISIJ Int.*, vol. 55, no. 4, pp. 904–906, 2015. DOI: 10.2355/isijinternational.55.904.

[10] B. Glaser, M. Görnerup, and D. Sichen, "Thermal modelling of the ladle preheating process," *Steel Res. Int.*, vol. 82, no. 12, pp. 1425–1434, 2011. DOI: 10.1002/srin.201100198.